



## Performance enhancement of polysulfone ultrafiltration membrane using TiO<sub>2</sub> nanofibers

Abhinav K. Nair, P.M. Shalin, P.E. JagadeeshBabu\*

*Department of Chemical Engineering, National Institute of Technology Karnataka, Surathkal, Mangalore 575 025, India, Tel. +91 8792706002; email: abhinav2411@yahoo.com (A.K. Nair), Tel. +91 9447754473; email: shalu505@yahoo.co.in (P.M. Shalin), Tel. +91 9632896086; Fax: +91 08242474057; emails: dr.jagadeesh@yahoo.co.in, jagadeesh78@nitk.ac.in (P.E. JagadeeshBabu)*

Received 4 November 2014; Accepted 27 March 2015

### ABSTRACT

Titanium dioxide nanofibers were synthesized via alkaline hydrothermal method using TiO<sub>2</sub> nanopowder. The hydrothermal method was optimized by studying the operating variables to obtain nanosized TiO<sub>2</sub> fibers. These nanofibers were used to make composite polysulfone ultrafiltration membranes along with polyethylene glycol as pore forming agent. The obtained samples were characterized using scanning electron microscope, X-ray diffraction, and attenuated total reflectance infrared spectroscopy. Contact angle measurements were used to estimate hydrophilicity of the membrane. Performance of the membrane was analyzed using pure water flux studies and antifouling studies with bovine serum albumin as the standard protein for rejection. The composite membranes exhibited better performance in both permeability and antifouling property.

*Keywords:* TiO<sub>2</sub> nanofibers; Polysulfone; Composite; Hydrophilicity; Antifouling

### 1. Introduction

Polysulfone (PSF) has been widely used as polymeric material for ultrafiltration membranes owing to its excellent chemical stability and mechanical properties [1]. The performance of a membrane generally depends on the wettability of the filtering medium. In water-based filtration processes, wettability depends on the hydrophilicity of the membrane. PSF is hydrophobic in nature and this result in poor flux and greater vulnerability to fouling [2]. Chemical surface treatment, blending with other polymers, and hydrophilic additives are some of the techniques that have been tried in the past to overcome hydrophobicity [3–5]. Polyethylene glycol (PEG) has been reported

as an additive to enhance permeation by improving the porosity of the membrane. PEG has also been reported to improve the dispersion of other additives [6,7]. But higher concentration of PEG results in poor rejection and mechanical behavior [8,9]. With the dawn of nanotechnology, nanocomposite membranes have gained much interest. Researchers have investigated PSF membranes incorporated with various nanoparticles and obtained enhanced performance [10,11].

Titanium dioxide nanomaterials find wide applications in the fields of photo voltaic cells, photo catalysis, plastics, paints, and pharmaceuticals. TiO<sub>2</sub> nanoparticles are hydrophilic in nature and are being functionalized with suitable functional group to convert it as hydrophobic nanoparticle. Conversely, these particles have been directly brought to use in membrane technology to improve hydrophilicity. TiO<sub>2</sub>

\*Corresponding author.

nanoparticles have been reported earlier as performance enhancement additives in PSF membranes [12]. These nanomaterials are nontoxic and possess catalytic activity, super-hydrophilicity, self cleaning property, and bacterial resistance [13,14]. Titanium dioxide nanofiber (TNF) is one among the different morphological forms of titanium dioxide nanomaterials. TNF being in fiber form has an edge over the others due to its higher specific surface area; which in turn results in greater interfacial area in composites [15]. TNF can hence serve as a better reinforcing material in composites due to greater interface interaction; lesser quantity of additive can thus bring about better property enhancement [16]. Based on the literature survey TNF in PSF has not been reported yet. In this study, titanium dioxide nanofibers were synthesized via alkaline hydrothermal treatment method by optimizing the various operating variables [17]. The synthesized fibers were characterized and used as additives in PSF casting solutions to make composite membranes with different compositions. Membranes were characterized using scanning electron microscope (SEM), X-ray diffraction (XRD), and attenuated total reflectance infrared (ATR-IR). Contact angle measurements were made to evaluate membrane hydrophilicity. The performance of these membranes was evaluated using pure water flux (PWF) and antifouling studies using bovine serum albumin (BSA) as a standard protein for rejection [18,19].

## 2. Experimental process

### 2.1. Materials

PSF with molecular weight 35,000 Da, Titanium (IV) oxide ( $\text{TiO}_2$ ) nanopowder (particle size 21 nm), and Bradford reagent were purchased from Sigma-Aldrich Co, Bangalore, India. 1-Methyl-2-pyrrolidone (NMP), polyethylene glycol (PEG) 600, ethanol, sodium hydroxide (NaOH), hydrochloric acid (HCl, 37%), and ammonium hydroxide were purchased from Merck, India Ltd. BSA was purchased from Central Drug House (CDH), New Delhi, India. All the chemicals were used without further purification process.

### 2.2. Synthesis of TNF

In brief, 2.5 g of  $\text{TiO}_2$  nanopowder and 2-drops of span-80 surfactant was added to 300 mL of 12 M NaOH aqueous solution and stirred for 30 min. After stirring, the suspension was transferred in to a Teflon-lined stainless steel autoclave. The autoclave was kept in a hot air oven for three days at 170°C. The product obtained after hydrothermal treatment was washed

thoroughly with distilled water and then with dilute HCl (pH 2) till the pH became neutral. The nanofiber suspension was again washed with distilled water to remove NaCl content. Thus, obtained nanofibers were dried in a hot air oven for 24 h at 60°C and calcined at 500°C for 2 h in a muffle furnace.

### 2.3. Preparation of TNF incorporated PSF membranes

For preparation of M-1 membrane, PSF (20 wt.%), NMP (75 wt.%), and PEG (5 wt.%) were taken and kept for stirring at 60°C over a period of 4 h for complete dissolution of PSF to obtain a homogeneous solution. 1.0 wt.% of TNF (with respect to weight of polymer solution) was added to the solution at the same temperature and stirred for 30 min. The viscous solution was cast over a glass plate using a finely polished glass rod by maintaining a membrane thickness of 0.3 mm [19,20]. The glass plate was then immersed in distilled water (at 20°C) for phase inversion. A similar procedure was followed for the preparation of other membranes with compositions as shown in Table 1.

## 3. Characterization

### 3.1. ATR-IR analysis

The ATR-IR spectra of membranes were obtained using Jasco 4,200 IR Spectrometer in the range of 4,000–650  $\text{cm}^{-1}$ . The spectra of TNF and composite membranes were studied.

### 3.2. XRD analysis

XRD was done using Rigaku Miniflux 6000, X-ray diffractometer equipped with monochromatized high intensity  $\text{Cu K}\alpha$  radiation ( $\lambda = 1.54178 \text{ \AA}$ ). The diffractograms were obtained at 0.06°/s in the  $2\theta$  range 10°–60°.

### 3.3. SEM analysis

Jeol JSM-6380LA, SEM was used to obtain SEM images of nanofibers and membranes. The membrane samples were cryogenically fractured using liquid nitrogen before taking cross-sectional images. All samples were sputtered with gold before scanning.

### 3.4. Contact angle measurement

FTA-200 dynamic contact angle analyzer was used to estimate the contact angle of membranes using sessile

Table 1  
Blending compositions of membranes

Membranes	PSf (wt.%)	PEG (wt.%)	TNF (wt.%)	NMP (wt.%)	Viscosity (mPaS)
M-0	20	5	0	75	786
M-1	20	5	1	75	813
M-3	20	5	3	75	865
M-5	20	5	5	75	901
M-10	20	5	10	75	1,342

droplet method. In order to minimize experimental error the contact angle values were obtained as an average of three trials at different locations.

### 3.5. Permeation properties

Sterlitech HP4750 stirred dead end filtration cell with an effective membrane area of 14.6 cm<sup>2</sup> was used to study the performance of the membranes. Membranes were kept immersed in distilled water for 24 h before carrying out flux study. The time-dependent PWF of membrane was studied. The permeate sample collection was started after 20 min of exposure to 0.2 MPa transmembrane pressure (TMP) at 25°C and continued at every 5 min interval. The PWF ( $J_w$ ) was calculated using the following equation:

$$J_w = \frac{Q}{\Delta t A} \quad (1)$$

where  $J_w$  is expressed in L/m<sup>2</sup> h and  $Q$  is the amount of water collected for  $\Delta t$  (h) time duration using a membrane of area  $A$  (m<sup>2</sup>).

### 3.6. Antifouling properties

The antifouling property of the membrane was studied as per procedure reported in the literature [21]. In brief, initial PWF of the membrane  $J_{w1}$  (L/m<sup>2</sup> h) was obtained at 0.2 MPa TMP. The antifouling property of the membrane was studied using BSA as standard protein for rejection. An aqueous solution (0.8 g/L) of BSA was prepared and filtered through the membrane for 90 min. Later the membrane was flushed with distilled water for 20 min and PWF  $J_{w2}$  (L/m<sup>2</sup> h) was determined once again. The membrane antifouling property was estimated in terms of flux recovery ratio (FRR) using the following equation:

$$\text{FRR} (\%) = \frac{J_{w2}}{J_{w1}} \times 100 \quad (2)$$

In order to determine the rejection capacity of the membrane, feed and permeate solution samples were collected and treated with Bradford reagent. Samples were kept for 10 min before analyzing using UV spectrometer. The BSA percentage rejection of the membrane was determined using the following equation:

$$R\% = \left(1 - \frac{C_p}{C_f}\right) \times 100 \quad (3)$$

where  $C_p$  (mg/mL) and  $C_f$  (mg/mL) are the BSA concentrations in permeate and feed, respectively. The concentrations were measured using UV spectrophotometer at a wavelength of 595 nm.

## 4. Results and discussion

### 4.1. Synthesis and characterization of TiO<sub>2</sub> nanofibers

Optimized hydrothermal treatment yielded in TNFs with an average diameter of around 100 nm and length of 3–4 μm as shown in Fig. 1.

The ATR-IR spectrum of TNF is shown in Fig. 2(a). The peak at 894.8 cm<sup>-1</sup> corresponds to the longitudinal

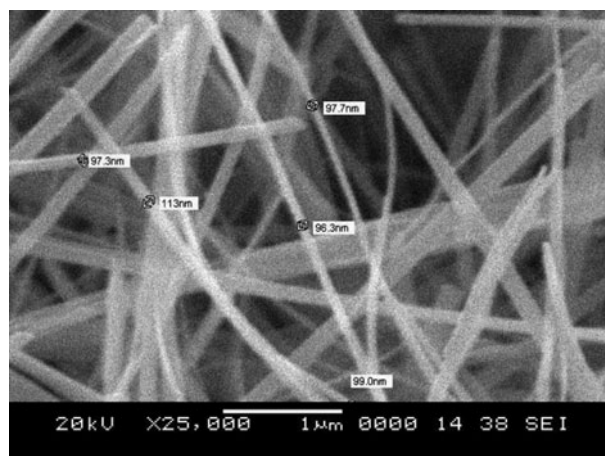


Fig. 1. SEM image of TNFs.

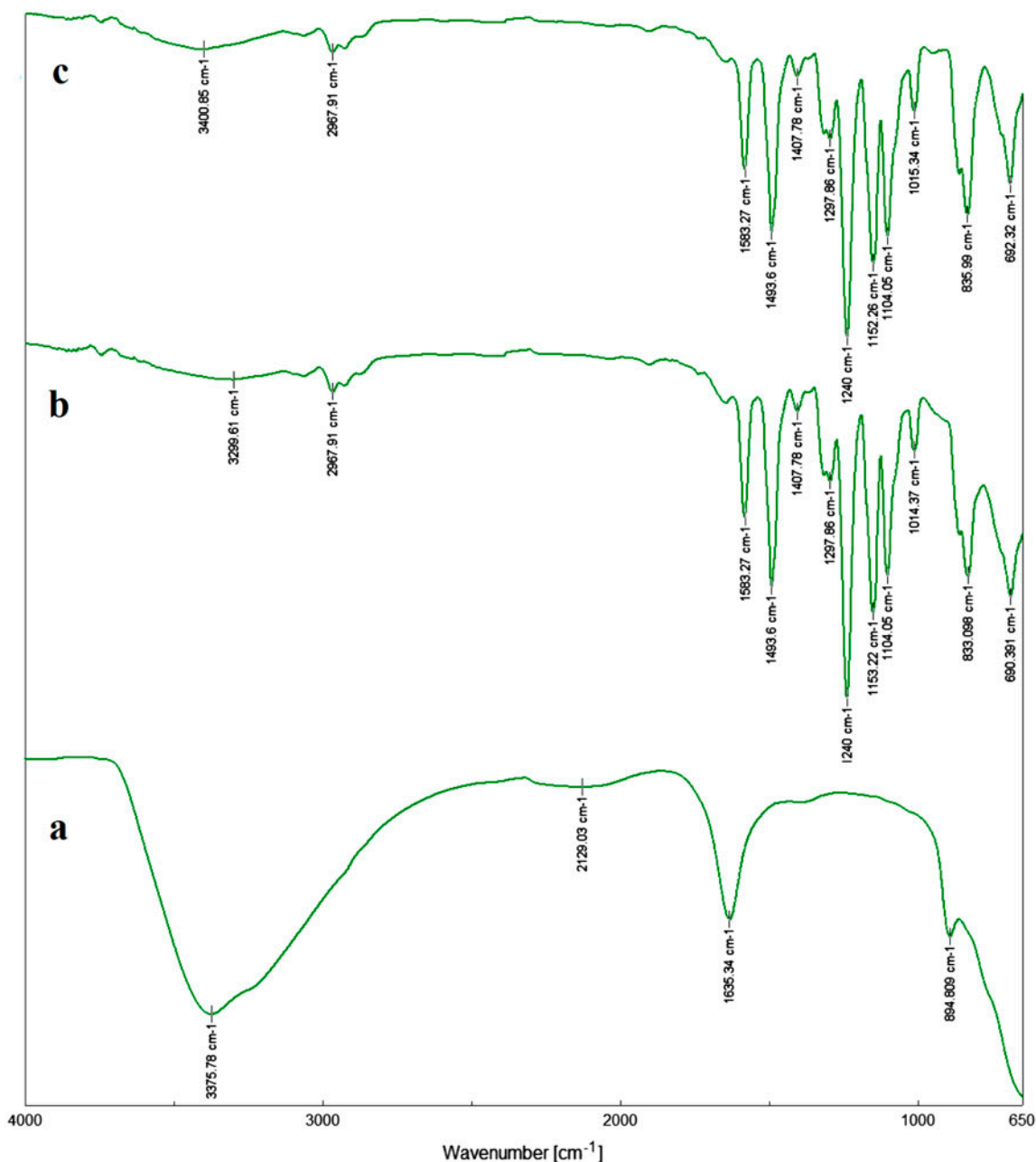


Fig. 2. ATR-IR spectra, (a) TNF; (b) M-0; (c) M-10.

optical mode of anatase phase of  $\text{TiO}_2$ . The presence of polymeric Ti–O chains in the nanofibers can be identified by lowering of transmittance beyond  $650\text{ cm}^{-1}$ . The broad peak around  $3,375\text{ cm}^{-1}$  corresponds to O–H vibrations of Ti–OH groups due to physisorbed water content [22]. The XRD pattern of the TNF is shown in Fig. 3. The characteristic peaks at  $25.4^\circ$ ,  $38.5^\circ$ ,  $48^\circ$ , and  $53.8^\circ$  in the powder diffraction pattern indicates majority of anatase phase content [23].

## 4.2. Membrane characterization

### 4.2.1. ATR-IR analysis

ATR-IR spectra of M-0, M-10, and TNF are compared in Fig. 2. The characteristic peaks of PSF at  $1,297.86\text{ cm}^{-1}$  (S=O asymmetric stretch),  $1,240\text{ cm}^{-1}$  (C–O–C stretch), and  $1,152.26\text{ cm}^{-1}$  (S=O symmetric stretch) can also be seen in the composite membrane [24]. Apart from the PSF peaks, a notable peak that appears in M-0 is the broad peak around  $3,400\text{ cm}^{-1}$

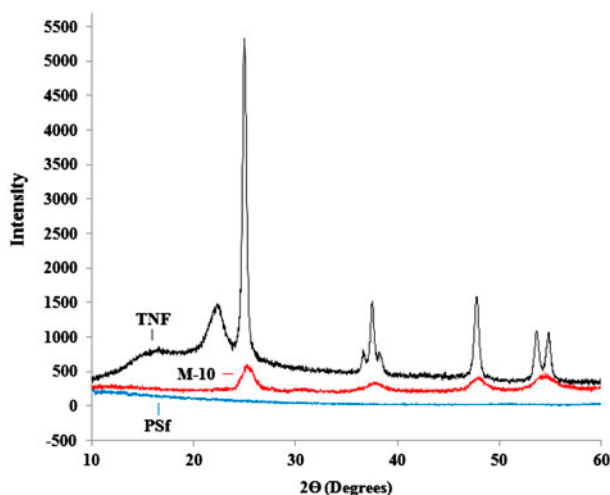


Fig. 3. XRD patterns of TNF, PSF, and M-10.

which is due to the incorporation of PEG [19]. The peaks in the TNF spectrum at  $3,375$  and  $650\text{ cm}^{-1}$  have got merged with the corresponding M-0 peaks in the region to give lower peaks at  $3,299$  and  $690\text{ cm}^{-1}$  in the M-10 spectrum. The merger of peaks implies good interaction between TNF and PSF. The broad  $-\text{OH}$  peak around  $3,300\text{--}3,400\text{ cm}^{-1}$  is of great importance as it gives an idea of interactions with in the composite and also about the dispersion of the additive. The significant diminution in  $-\text{OH}$  peak of M-10 when compared to pure TNF indicates towards the lowered polarizability of hydroxyl group within the polymer. When filler is polar and the polymer is non-polar then the filler–filler interaction is much stronger than polymer–filler interaction. Higher concentrations of filler thus result in agglomeration and non-uniform dispersion [25]. In the present work the inclusion of hydrophilic PEG with hydroxyl groups greatly helps in better dispersion even at higher concentrations of TNF.

#### 4.2.2. XRD analysis

The XRD pattern of TNF, M-0, and M-10 are compared in Fig. 3. XRD of M-0 shows no peaks indicating absence of any crystalline phase, affirmative in case of an amorphous polymer. Anatase characteristic peaks around  $25.4^\circ$ ,  $38.5^\circ$ ,  $48^\circ$ , and  $53.8^\circ$  in the powder diffraction pattern can be seen in the M-10 membrane at a lower intensity, the small shift in peaks indicates effective incorporation and good interaction between filler and matrix [12].

#### 4.2.3. Morphology of the membrane

SEM analysis of the cross section of membranes with different concentrations of TNF is shown in Fig. 4. The membranes depict asymmetric structure, typically the dense top layer, porous sub layer, and fully developed macro pores layer. It is apparent from SEM cross-sectional images that the raise in concentration of TNF resulted in a decrease in finger-like projection with reduced length [26]. The formation of porous structure in the sub-layer was favored with higher additive content. Viscosity of cast solution increases with rising additive content. This increased viscosity affects the kinetics of phase inversion as it retards the diffusion of solvent and non-solvent. The higher the solution viscosity, solvent's outdiffusion from the cast solution is favored over non-solvent's indiffusion into the solution resulting in the formation of membranes with smaller pores [27]. In case of  $\text{TiO}_2$  nanoparticles there are reports of increased rheological hindrance beyond the rheological percolation threshold with increasing concentration of additive [12]. The increased hydrophilicity due to the hydrophilic additive favors indiffusion of water, and thus plays an important role in overcoming the increase in rheological hindrance. There are also reports where addition of  $\text{TiO}_2$  nanoparticles even at higher concentrations did not result in lower pore size or reduced flux [28,29]. In this context the addition of PEG would play a significant role apart from being a hydrophilic pore former, it also improves the dispersion and interaction between the polar TNF and non-polar PSF during membrane formation as understood from ATR-IR spectra [25]. With increasing concentration, nano-additive can get trapped in the pores and block them. But when small concentration of PEG is added the additives get dispersed mainly in the polymer matrix [7].

#### 4.2.4. Hydrophilicity of membranes

Hydrophilicity of the membranes active surface is the key factor in determining the flux and antifouling properties of the membrane. Contact angle measurement is a viable tool to study surface hydrophilicity of the membrane [30]. As hydrophilicity of membrane increases, the surface wettability of the membrane will increase, which will result in decrease in the contact angle. From the analysis (Fig. 5), it was observed that the contact angle of TNF blend PSF membranes gradually reduced from  $73.88^\circ$  for 0 wt.% TNF content to  $48.88^\circ$  for the 10 wt.% TNF content. The significant drop-off in contact angle with increasing concentration of TNF is an obvious sign of improving hydrophilicity

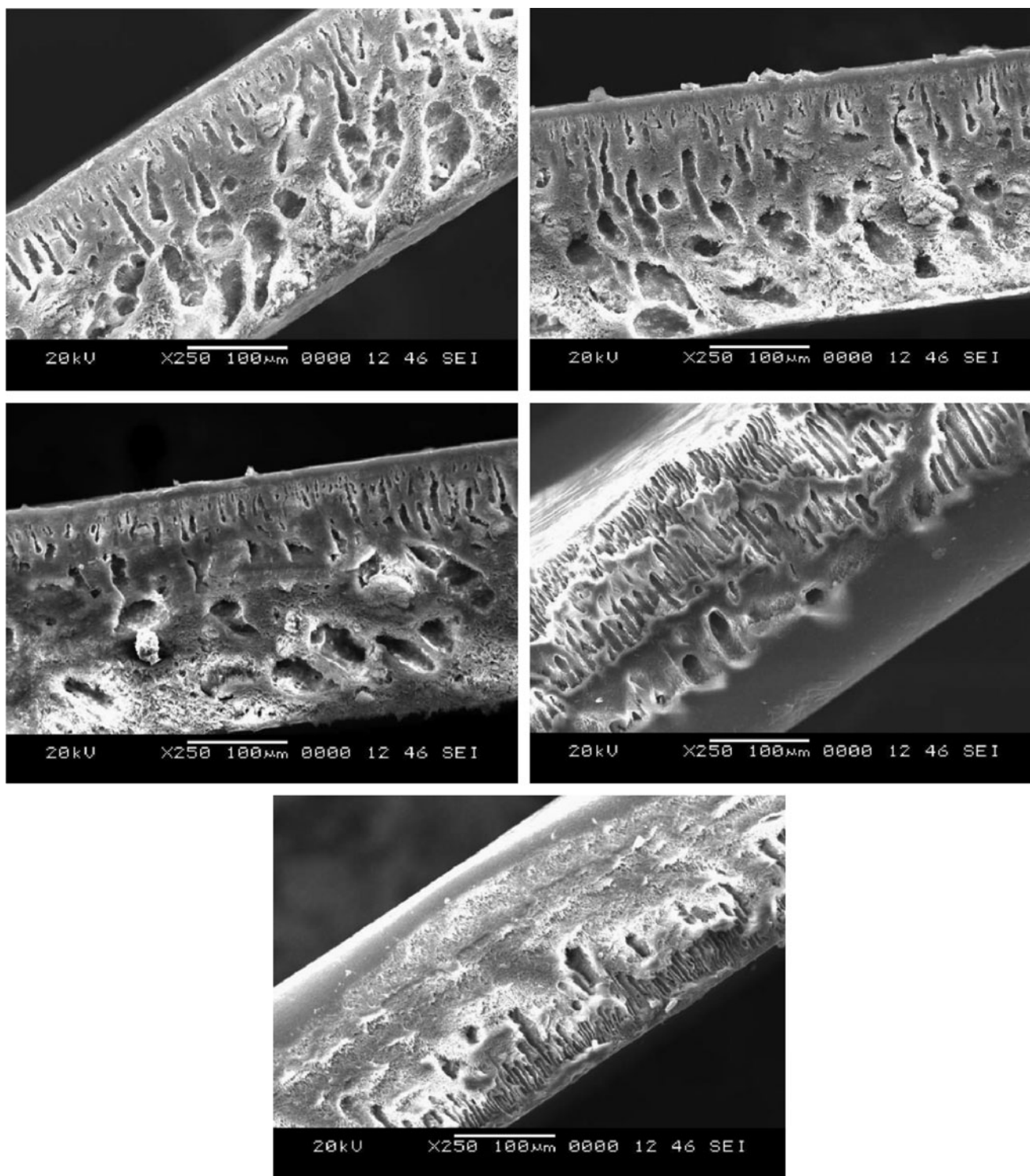


Fig. 4. Cross-sectional SEM images of membranes, (a) M-0; (b) M-1; (c) M-3; (d) M-5; (e) M-10.

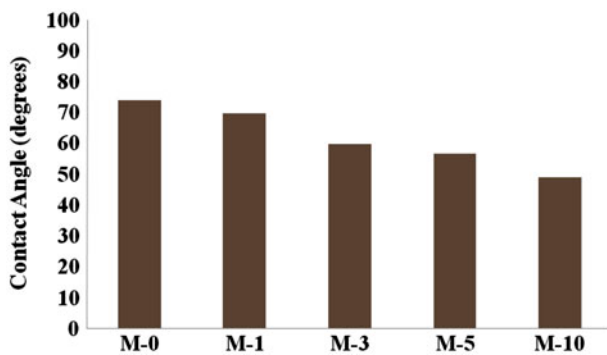


Fig. 5. Contact angle measurements of the membranes.

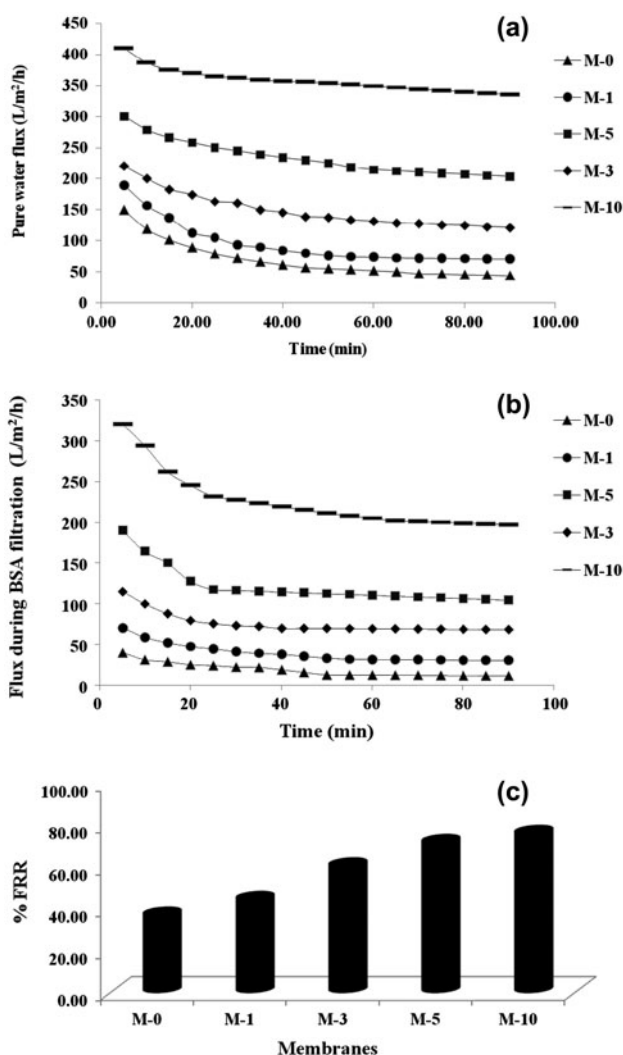


Fig. 6. Permeation and antifouling studies of the membranes, (a) The PWF; (b) flux during BSA rejection; (c) flux recovery.

of the membranes [31]. It can be concluded that the increase in the hydrophilicity could be due to the hydrophilicity of TNF additive.

#### 4.2.5. Membrane permeability and antifouling properties

Membrane performance was evaluated in terms of time dependent PWF, BSA rejection, and flux recovery after BSA rejection. Initially, all membranes showed flux decline during PWF due to mechanical compaction [32]. Flux study i.e. PWF, flux during BSA rejection and the recovered flux were carried out at 0.2 Mpa TMP and 25°C for 90 min till the flux reached nearly steady state condition. The PWF flux of different membranes is compared in Fig. 6(a). The study showed an increasing trend in PWF with increasing TNF concentration.

The ever-increasing trend in flux is an indication of better dispersion of TNF in the membrane, and it is also an indication of minimal trapping of TNFs in the pores [7]. The enhanced hydrophilicity of membranes due to addition of TNF is the key reason for the enhancement of permeability.

Fouling is a major drawback in PSF membranes due to the hydrophobic interaction between the membrane surface and the foulant [19]. Fouling leads to flux reduction and reduces membrane lifetime. It was observed that although all membranes showed similar trends of flux reduction during BSA rejection, lesser flux reduction was observed with increasing TNF concentration in the membrane (Fig. 6(b)). The BSA rejection values of M-0, M-1, M-3, M-5, and M-10 membranes were 94, 92, 90, 89, and 86%, respectively. All TNF incorporated membranes showed higher FRR values than PSF membrane. The maximum FRR of 76% was observed in M-10 membrane with 10% of TNF nanoparticles. The hydrophilic TNF on the membrane surface improved the interaction with aqueous medium thus weakening interactions between membrane surface and protein molecules. This enables easy cleansing of foulant from the membrane surface, greatly enhancing the recyclability of the membranes.

## 5. Conclusions

Titanium oxide nanofibers were successfully synthesized within the range of 90–100 nm diameters. PSF/TNF composite membranes were successfully synthesized and characterized using SEM, XRD, ATR-IR, and contact angle measurements. The performance of membrane was analyzed using PWF, FRR, and percentage rejection. The membranes were found to

possess an asymmetric structure as observed from cross-sectional SEM images. Contact angle measurements indicated a clear increase in membrane hydrophilicity with increasing concentration of TNF content. The PSF/TNF composite membranes showed better permeability than nascent PSF membrane. The membrane with 10 wt.% addition of TNF showed the highest value for PWF. Lower flux declination was observed for the composite membranes during BSA rejection. The antifouling study showed improved results with greater concentration of TNF. 10 wt.% TNF addition recorded a maximum FRR of 76%.

### Acknowledgments

The authors thank Prof. K. Narayan Prabhu, Metallurgical and Materials Engineering Department of NITK Surathkal, India for providing contact angle measurement facility. They also thank Dr. Anandhan Srinivasan, Associate professor, Metallurgical and Materials Engineering Department of NITK Surathkal, India for providing ATR-IR facility.

### Symbols

$J_w$	—	flux of pure water (L/m <sup>2</sup> h)
$A$	—	cross section area of membrane (m <sup>2</sup> )
$Q$	—	amount of permeate collected (L)
$\Delta t$	—	time duration (h)
FRR%	—	flux recovery ratio (%)
R%	—	% BSA rejection
$C_p$	—	BSA concentrations in permeate (mg/mL)
$C_f$	—	BSA concentrations in feed (mg/mL)

### References

- [1] F. Mahmoudi, E. Saljoughi, Promotion of polysulfone membrane by thermal–mechanical stretching process, *J. Polym. Res.* 20(96) (2013) 1–10.
- [2] M.K. Sinha, M.K. Purkait, Increase in hydrophilicity of polysulfone membrane using polyethylene glycol methyl ether, *J. Membr. Sci.* 437 (2013) 7–16.
- [3] T.D. Santos, K.A. Pacheco, P. Poletto, C.S. Meireles, A.M.C. Grisa, M. Zeni, Effect of cellulose fibers on morphology and pure water permeation of PSf membranes, *Desalin. Water Treat.* 27 (2012) 1–3.
- [4] R. Kumar, A.M. Isloor, A.F. Ismail, T. Matsuura, Performance improvement of polysulfone ultrafiltration membrane using N-succinyl chitosan as additive, *Desalination* 318 (2013) 1–8.
- [5] R. Kumar, A.M. Isloor, A.F. Ismail, T. Matsuura, Synthesis and characterization of novel water soluble derivative of Chitosan as an additive for polysulfone ultrafiltration membrane, *J. Membr. Sci.* 440 (2013) 140–147.
- [6] Y. Ma, F. Shi, Z. Wang, M. Wu, J. Ma, C. Gao, Preparation and characterization of PSf/clay nanocomposite membranes with PEG 400 as a pore forming additive, *Desalination* 286 (2012) 131–137.
- [7] C. Dong, G. He, H. Li, R. Zhao, Y. Han, Y. Deng, Antifouling enhancement of poly (vinylidene fluoride) microfiltration membrane by adding Mg(OH)<sub>2</sub> nanoparticles, *J. Membr. Sci.* 387–388 (2012) 40–47.
- [8] Y. Ma, F. Shi, J. Ma, M. Wu, J. Zhang, C. Gao, Effect of PEG additive on the morphology and performance of polysulfone ultrafiltration membranes, *Desalination* 272 (2011) 51–58.
- [9] J. Kim, K. Lee, Effect of PEG additive on membrane formation by phase inversion, *J. Membr. Sci.* 138 (1998) 153–163.
- [10] X. Zhang, B. Shi, X. Liu, Preparation of polysulfone ultrafiltration membranes modified by silver particles, *Desalin. Water Treat.* 51 (2012) 19–21.
- [11] A.L. Ahmad, M.A. Majid, B.S. Ooi, Functionalized PSf/SiO<sub>2</sub> nanocomposite membrane for oil-in-water emulsion separation, *Desalination* 268 (2011) 266–269.
- [12] Y. Yang, H. Zhang, P. Wang, Q. Zheng, The influence of nano-sized TiO<sub>2</sub> fillers on the morphologies and properties of PSF UF membrane, *J. Membr. Sci.* 288 (2007) 231–238.
- [13] H. Zhao, H. Li, H. Yu, H. Chang, X. Quan, S. Chen, CNTs-TiO<sub>2</sub>/Al<sub>2</sub>O<sub>3</sub> composite membrane with a photocatalytic function: Fabrication and energetic performance in water treatment, *Sep. Purif. Technol.* 116 (2013) 360–365.
- [14] R. Vinodh, K. Aravind Bhat, Fabrication, characterization and invitro bioactivity evaluation of QPSU/TiO<sub>2</sub> composite membranes, *J. Polym. Res.* 18 (2011) 1469–1477.
- [15] G. He, Y. Cai, Y. Zhao, X. Wang, C. Lai, M. Xi, Electrospun anatase-phase TiO<sub>2</sub> nanofibers with different morphological structures and specific surface areas, *J. Colloid Interface Sci.* 398 (2013) 103–111.
- [16] A.A. Gawandi, J.M. Whitney, G.P. Tandon, R.B. Brockman, Three-dimensional analysis of the interaction between a matrix crack and nanofiber, *Composites Part B* 40 (2009) 698–704.
- [17] Z. Yuan, B. Su, Titanium oxide nanotubes, nanofibers and nanowires, *Colloids Surf., A* 241 (2004) 173–183.
- [18] A. Nabe, E. Staude, G. Belfort, Surface modification of polysulfone ultrafiltration membranes and fouling by BSA solutions, *J. Membr. Sci.* 133 (1997) 57–72.
- [19] A.K. Nair, A.M. Isloor, R. Kumar, A.F. Ismail, Antifouling and performance enhancement of polysulfone ultrafiltration membranes using CaCO<sub>3</sub> nanoparticles, *Desalination* 322 (2013) 69–75.
- [20] B.M. Ganesh, A.M. Isloor, M. Padaki, Preparation and characterization of polysulfone and modified poly isobutylene-alt-maleic anhydride blend NF membrane, *Desalination* 287 (2012) 103–108.
- [21] S. Zhao, Z. Wang, X. Wei, B. Zhao, J. Wang, Performance improvement of polysulfone ultrafiltration membrane using PANiEB as both pore forming agent and hydrophilic modifier, *J. Membr. Sci.* 385–386 (2011) 251–262.
- [22] M. Reza, H. Abdizadeh, Effects of acid catalyst type on structural, morphological, and optoelectrical properties of spin-coated TiO<sub>2</sub> thin film, *Phys. B Phys. Condens. Matter* 413 (2013) 40–46.

- [23] A. Zaleska, E. Kowalska, T. Klimczuk, TiO<sub>2</sub> photoactivity in vis and UV light: The influence of calcination temperature and surface properties, *Appl. Catal. B* 84 (2008) 440–447.
- [24] R. Kumar, A.F. Ismail, M.A. Kassim, A.M. Isloor, Modification of PSf/PIAM membrane for improved desalination applications using Chitosan coagulation media, *Desalination* 317 (2013) 08–115.
- [25] G. George, A. Mahendran, S. Anandhan, Use of nano-ATH as a multi-functional additive for poly(ethylene-co-vinyl acetate-co-carbon monoxide), *Polym. Bull.* 71 (2014) 2081–2102.
- [26] B. Singh, V. Kochkodan, R. Hashaikeh, N. Hilal, A review on membrane fabrication: Structure, properties and performance relationship, *Desalination* 326 (2013) 77–95.
- [27] J.-H. Choi, J. Jegal, W.-N. Kim, Fabrication and characterization of multi-walled carbon nanotubes/polymer blend membranes, *J. Membr. Sci.* 284 (2006) 406–415.
- [28] X. Zhang, Y. Wang, Y. You, H. Meng, J. Zhang, X. Xu, Effect of TiO<sub>2</sub> nanoparticle size on the performance of PVDF membrane, *Appl. Surf. Sci.* 253 (2006) 2003–2010.
- [29] X.-M. Wang, X.-Y. Li, K. Shih, In situ embedment and growth of anhydrous and hydrated aluminum oxide particles on polyvinylidene fluoride (PVDF) membranes, *J. Membr. Sci.* 368 (2011) 134–143.
- [30] A. Sotto, A. Marti, S.B. Teli, J. De Abajo, Influence of the type, size, and distribution of metal oxide particles on the properties of nanocomposite ultrafiltration membranes, *J. Membr. Sci.* 428 (2013) 131–141.
- [31] V.E. Reinsch, A.R. Greenberg, S.S. Kelley, R. Peterson, L.J. Bond, A new technique for the simultaneous, real-time measurement of membrane compaction and performance during exposure to high-pressure gas, *J. Membr. Sci.* 171 (2000) 217–228.
- [32] S.B. Teli, S. Molina, E.G. Calvo, A.E. Lozano, J. de Abajo, Preparation, characterization and antifouling property of polyethersulfone-PANI/PMA ultrafiltration membranes, *Desalination* 299 (2012) 113–122.